

Designer quantum states of matter created atom-by-atom

Alexander A. Khajetoorians^{1,*}, Daniel Wegner¹, Alexander F. Otte², Ingmar Swart^{3,#}

¹*Scanning Probe Microscopy Department, Institute of Molecules and Materials, Radboud University, Nijmegen, The Netherlands*

²*Department of Quantum Nanoscience, Kavli Institute of Nanoscience, Delft University of Technology, Delft, The Netherlands*

³*Debye Institute for Nanomaterials Science, Utrecht University, Utrecht, The Netherlands*

[*a.khajetoorians@science.ru.nl](mailto:a.khajetoorians@science.ru.nl)

[#I.Swart@uu.nl](mailto:I.Swart@uu.nl)

With the advances in high resolution and spin-resolved scanning tunneling microscopy as well as atomic-scale manipulation, it has become possible to create and characterize quantum states of matter bottom-up, atom-by-atom. This is largely based on controlling the particle- or wave-like nature of electrons, as well as the interactions between spins, electrons, and orbitals and their interplay with structure and dimensionality. We review the recent advances in creating artificial electronic and spin lattices that lead to various exotic quantum phases of matter, ranging from topological Dirac dispersion to complex magnetic order. We also project future perspectives in non-equilibrium dynamics, prototype technologies, engineered quantum phase transitions and topology, as well as the evolution of complexity from simplicity in this newly developing field.

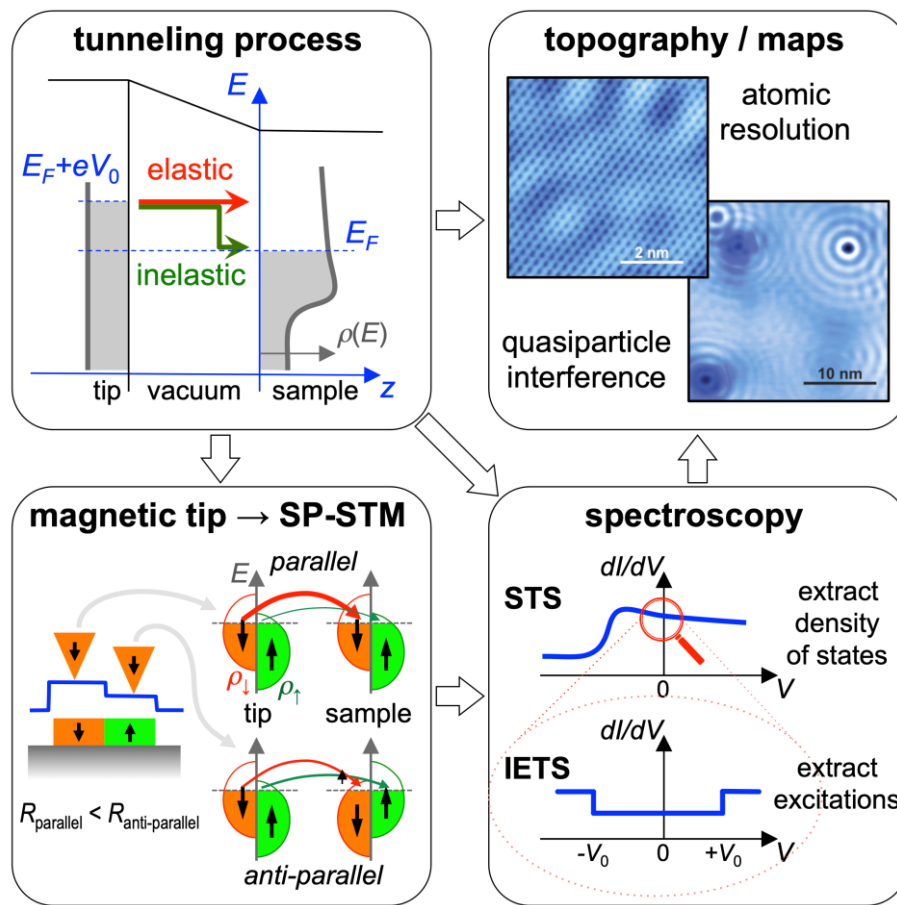
Introduction

One promising route toward understanding novel quantum states of matter is to engineer many-body states, from the bottom-up, in so-called artificial lattices. 2D artificial lattices can serve as model systems to realize various properties seen in 3D, with the advantage that all the relevant interactions can be controlled, serving as an ideal model system for theoretical innovation³⁻⁵. The concept behind artificial lattices is building up periodic structures where symmetry and interactions, for example between collections of electrons and/or spins, are precisely tailored^{3,6}. Artificial lattices have been realized in vastly different experimental communities, e.g. cold atoms⁸, trapped ions¹⁰, superconducting circuits¹³, patterned devices¹⁵, optical lattices^{16,17}, and most recently twisted bilayer graphene^{18,19}. Since novel quantum states of matter arise in certain well-defined arrangements of atoms, it is natural to develop platforms that allow the creation and manipulation of quantum matter on

the atomic scale with a high degree of tunability, simultaneously enabling characterization with high precision.

The ultimate flexibility is to realize an experiment that combines *in-situ* construction of an electron or spin lattice with a chosen geometry and with atomic-level control of the relevant interactions, while having the simultaneous ability to probe the changes in the electronic and magnetic properties. To this end, atomically precise structures have been created using self-assembly and on-surface chemistry²⁰⁻²³, where the properties of the final material (which can be the molecular network itself or the surface patterned into an array of quantum confinements) are encoded in the precursor species used. Key strategies are based on utilization of tailored intermolecular interactions (e.g. hydrogen and halogen bonding)²⁴⁻²⁸, the formation of metal-organic coordination bonds (e.g. using functional cyano or carboxylate groups)^{23,28-31}, or on-surface polymerization (e.g. utilizing Ullmann-type reactions)^{22,32-35}. An advantage of utilizing self-assembly and self-organization is that large artificial structures can be created quickly. A disadvantage is the reduced flexibility in tuning different structures using the same building blocks, and controlled construction of lateral artificial heterostructures remains difficult. Likewise, incorporation of specific atomically precise defects, as well as the number and spacing of these defects is not possible. Moreover, only few studies thus far focused on tailoring and studying the electronic or spin structure of self-assembled artificial lattices^{24,25,27,34,35}. An alternative, especially appealing approach to study quantum matter with ultimate flexibility and precision is artificial lattices derived from patterned atomic impurities, created and probed by scanning tunneling microscopy (STM).^{3-5,36} To date, this concept has been utilized to realize many novel states of matter, ranging from lower-dimensional Bloch states toward Dirac materials such as artificial graphene³ and the Lieb lattice^{4,5}, as well as a variety of tailored nanomagnets with designed magnetic order^{6,37-40}. This review will hence focus on artificial electronic and spin lattices created by STM-based atomic manipulation. Low-temperature STM has become a powerful tool to both create *and* characterize quantum matter at the atomic scale⁴¹. Tailoring electronic and magnetic properties with single atoms has a long history^{6,38,42,43}, stemming from the first quantum corral built in 1993 at IBM Almaden⁴³ (see info box 2). Since that time, there has been an exhibition of ground-breaking examples, in which manipulated structures have led to new understandings of magnetism, as well as prototype technologies^{6,37,38,44,45}. Scanning tunneling spectroscopy (STS) gives access to the density of states, and in combination with

Box 1: The scanning tunneling microscope – an integrated nanolab



Since its invention and demonstration of atomic resolution by Binnig and Rohrer, the STM has developed into a versatile tool reaching far beyond mere imaging of surfaces, mostly owing to the implementation into cryogenic ultrahigh vacuum environments⁵¹. Performing STM at low temperatures not only freezes adatom diffusion but also inhibits thermal drift between the STM tip and the sample, permitting to position and stabilize the tip over an atomic site for weeks. This high stability is also the basis for the STM's capability to manipulate single adsorbates (atoms or molecules) or surface vacancies with atomic-scale precision (see Box 2).

The vast success of cryogenic STM is further based on scanning tunneling spectroscopy (STS), where the tunnel current I is measured as a function of applied sample bias V under open-feedback conditions^{52,53}. The differential conductance dI/dV is, in good approximation, proportional to the sample's electronic local density of states, allowing to probe both occupied ($V < 0$) and unoccupied ($V > 0$) states. Here, the energy resolution is directly proportional to the temperature ($\Delta E \approx 3.5 k_B T$), i.e. resolutions of 1-2 meV can be reached with conventional LHe bath cryostat systems, while state-of-the-art $^3\text{He}/^4\text{He}$ dilution refrigerator-based systems have shown resolutions more than one order of magnitude better⁵⁴⁻⁶⁰. Moreover, inelastic electron tunneling spectroscopy (IETS)⁶¹⁻⁶³ can be applied on the local scale in STM in order to excite molecular vibrations⁶⁴, phonons^{65,66}, spin excitations⁴⁶ or magnons⁶⁷. The classic hallmark of IETS is two symmetric steps around $V = 0$ in dI/dV at the resonance energy E_0 . The inelastic tunneling leads to mode excitation via energy loss and a lower final-state energy of the tunneling electron, hence opening an additional tunneling channel which leads to a sudden change of conductance at $V_0 = \pm E_0/e$.

A final key ingredient expanding the possibilities of STM is tip functionalization. The most influential type of functionalization is the use of a magnetic tip, by either using a bulk magnetic tip, by coating a nonmagnetic tip with a thin (anti-) ferromagnetic film, or by transferring a single magnetic atom onto the tip in an external magnetic field⁶⁸. The spin-polarized STM technique (SP-STM) is based on the fact that the spin of elastically tunneling electrons is conserved^{69,70}. If the tip and sample density of states are spin-polarized, this leads to a tunneling magnetoresistance and the tunnel current gives information on the projected local sample magnetization onto the polarization of the tip's last apex atom, hence enabling magnetic contrast with atomic resolution.

magnetic fields, it has been possible to observe topological superconductivity, Landau quantization in novel materials, and excitations of atomic spins with ultimate spatial resolution⁴⁶⁻⁴⁹. The advancements in atomic manipulation and automation^{42,50}, as well as ultra-high resolution and spin-sensitive scanning tunneling spectroscopy down to mK temperatures (see info box 1), has opened up the possibility to create quantum matter with designed properties and probe these states with atomic-scale resolution in and out of equilibrium. This combination provides the advantage of being able to combine fabrication, tailoring of individual interactions, and subsequent characterization in one seamless experiment.

Methods

Platforms for the realization of artificial lattices

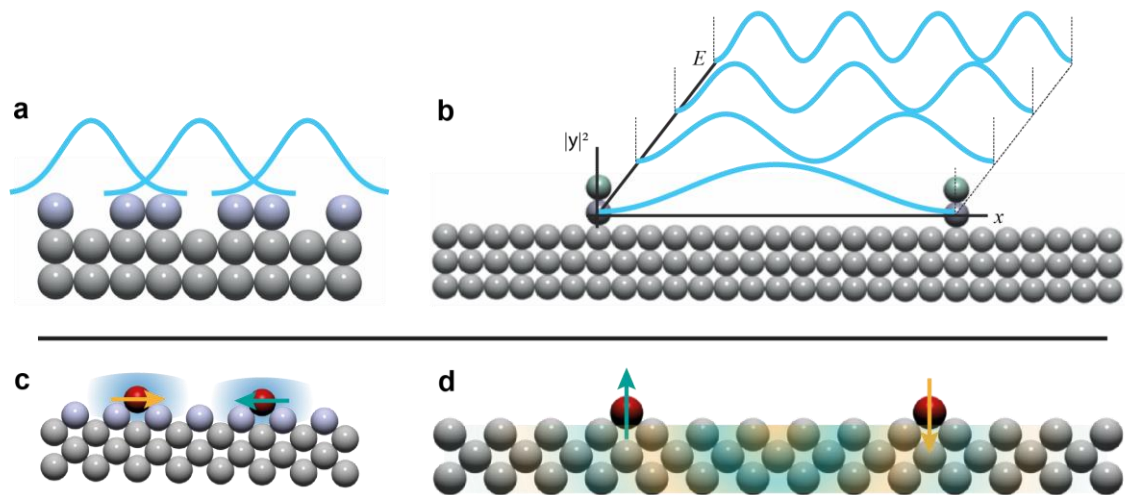


Fig. 1. Platforms for artificial electronic and spin lattices. Two different concepts can be applied based on either localized (left) or delocalized (right) interactions, for both electronic (top) and spin (bottom) lattices. (a) Tight-binding approach utilizing nearest-neighbour overlap of adsorbate orbitals or, as shown here, vacancy states. (b) Nearly free electron approach using 2D electron gases confined and restructured by adsorbates that serve as scattering centres. Bottom panel: spin lattice concepts. (c) Nearest-neighbour direct or superexchange of localized spins. (d) Long-range RKKY-like exchange interaction mediated by delocalized conduction band electrons.

There are two complementary models to describe the electronic structure of artificial lattices, namely the tight-binding and the nearly free electron model. Material platforms that mimic each of the two approaches are available for analogue quantum simulation experiments in a scanning tunneling microscope. As the tight-binding model is based on the coupling of atomic orbitals centred at

individual sites, structures assembled from closely bound atoms adsorbed on the surface are naturally described using this approach. A second material platform that is reminiscent of the tight-binding model are lattices made of Cl vacancies in NaCl/Cu(111)⁸⁴ and in Cl/Cu(100)⁴² (Fig. 1a). The electronic state associated with a vacancy can couple to that of a neighbouring vacancy in the same way as orbitals located on close-by atoms can couple.

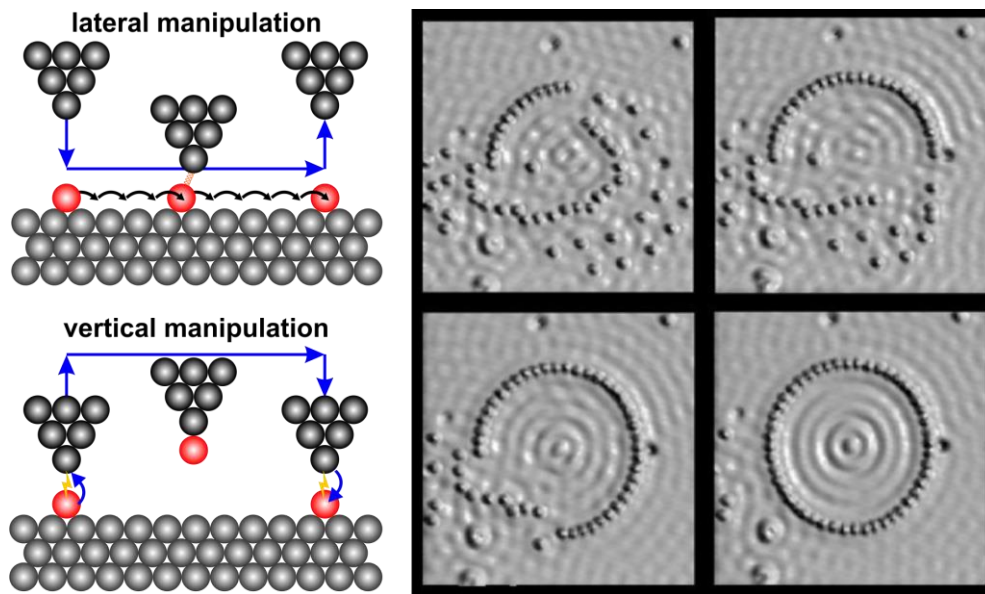
The nearly free electron model is best suited to describe artificial lattices created by patterning periodic scattering potentials on a 2D electron gas. The most prominent example of a 2D electron gas in STM literature is the Shockley surface state existing on several (111) noble metal surfaces. These surfaces typically host strong quasi-particle interference^{85,86} (Fig. 1b). By positioning intentionally introduced surface adsorbates, the 2D electron gas can be scattered and ultimately confined into nearly any geometry defined by the manipulated pattern, as we discuss below. To illustrate the conceptual link between the nearly free electron and the tight-binding models, consider the formation of a ring of metal adatoms on Cu(111) leading to the confinement of the surface state electrons inside the ring (see Box 2)^{74,87}. These so-called quantum corrals can either be thought of as particle-in-a-box systems (nearly free-electron model) or as 2D artificial atoms (tight-binding picture). Similarly, coupled quantum corrals and lattices created by patterning a 2D electron gas can be described both using both pictures.

A similar division can be made between two opposing regimes in coupled spin lattices, where the comparable parameter is the coupling strength between individual interacting spins, which is tuned by interatomic separation. The analogue of the tight-binding regime would be the case where individual localized spin states are coupled via nearest-neighbour exchange interactions only, i.e. via direct exchange or superexchange (Fig. 1c). The experimental systems that come closest to this limit are Fe atoms residing at next nearest neighbour sites on metallic surfaces^{47,88}, as well as the assembly of magnetic adatoms decoupled by an ultrathin insulating film from the conduction electrons in the underlying metal. On Cu₂N/Cu(100), transition metal atoms are incorporated into the surface molecular network through which superexchange interactions are mediated^{89,90}.

The spin-analogue of the nearly free electron model is the situation where the conduction electrons form a continuous spin bath that can mediate correlations between localized spins over a long distance (Fig. 1d). This indirect exchange, or so-called Ruderman-Kittel-Kasuya-Yosida (RKKY) interaction, plays a dominant role when magnetic atoms are placed directly atop a metal surface^{1,6,91}

with larger interatomic separation. It should be noted that the above division cannot be enforced very strictly in the material systems discussed here. Even for atoms on thin insulators, RKKY interactions are considered to play a sizable role. More prominent still is the role of magnetic anisotropy and Kondo screening, which can result in correlated states across multiple lattice sites if the atoms are placed sufficiently close⁹².

Box 2: Atom manipulation – controlling matter one atom at a time



Atomic manipulation is based on the principle that there is a force between the STM tip and the adsorbate when the tip is brought very close. In case of lateral manipulation of atoms or molecules, the tip is first lowered to the adsorbate via reduction of the tunneling resistance, and then moved laterally along the surface. In this regime, the force between the tip and the adsorbate is strong enough to overcome the surface diffusion barrier^{51,71,72}. The prototypical case for adatoms on metal surfaces exhibits an attractive tip-adsorbate force, i.e., the adsorbate follows the lateral motion of the tip, which is referred to as pulling or sliding mode^{71,73} (see, e.g., the construction of a quantum corral in the figure⁷⁴). In case of repulsive forces (pushing mode), the direction of adsorbate movement is less well controlled, but on a surface with anisotropic diffusion barriers this mode is also very useful⁷¹. In case of vertical manipulation, the adsorbate is reversibly transferred to the tip and back to the sample using voltage pulses with opposite polarity^{75,76}. This mode has the advantage that it allows for adsorbate transfer over very large distances as well as over obstacles such as step edges⁷⁶. Furthermore, it works on decoupling layers where lateral manipulation usually cannot be applied³⁷. Atomic manipulation can also be automated, allowing the creation of arbitrary artificial structures with atomic-scale precision^{5,50}. A hybrid form of these manipulation techniques is the local application of voltage (or current) pulses, which can induce single-step motion of adsorbates⁷⁷. This strategy is also applied for tip-induced desorption of adsorbates to artificially structure a surface, e.g. local dehydrogenation of H-passivated Si surfaces^{11,78}. We note that atom manipulation has also been demonstrated using inelastic tunneling processes^{77,79} and atomic force microscopy (AFM)^{72,80}. More information about atomic manipulation can be found in several review articles^{73,81-83}.

Artificial Electronic Lattices

In artificially constructed electronic systems it is possible to control the geometry and interaction strength of the artificial atoms in order to study the effects of coupling, topology, strain, periodicity (or lack thereof) and dimensionality. In this section, we will discuss examples of how these degrees of freedom have been used to realize various quantum states of matter.

After the construction of the quantum corral (cf. Box 2) and quantum mirage, which demonstrated the ability to tailor quantum confinement^{43,93}, one of the first phenomena to be studied bottom-up with atomic manipulation was the evolution of electronic band structure, from the limit of a single atom to extended chains (Fig. 2). One characteristic of quantum confinement in reduced dimensions is the appearance of quantum well states (QWS), where the dispersion of the states is discretized and depends on the confinement potential derived from the lattice constant in the direction of confinement. The appearance of the QWS can be probed as the structure is built. QWS built bottom-up have been investigated in a variety of manipulated chains derived from coupled adatoms on metallic, nearly insulating, and semiconducting surfaces^{2,7,94-99}. Moreover, induced atomic-scale defects, which exhibit a degree of charge localization, have also been utilized to create QWS, for example from dangling bonds derived from dehydrogenated silicon atoms¹¹ and by controllably coupled Cl vacancies^{4,14}. A characteristic example is shown in Fig. 2a, where the emergence of QWS can be seen for coupled Cu atoms on a Cu(111) surface. All experiments on metal adatoms on metal surfaces provide qualitatively the same results^{2,94-96,99}, suggesting that the exact nature of the metal adatoms and metal substrate are not important.

In contrast to metallic surfaces, for coupled adatoms on semiconductors, both direct coupling between adsorbates (Fig. 2b), as well as complex site-specific hybridization of adatoms⁹⁸ and substrate-derived states (chains created via self-assembly)¹⁰⁰ have been observed. By assembling chains along different crystallographic directions of a substrate, it is possible to control the distance between the metal adatoms and therefore the hopping parameter between the adatoms⁹⁷. As expected, an increased nearest-neighbor distance results in less coupling and smaller energy level spacing as well as an increased effective electron mass. The conclusions drawn from the work on adatom chains are supported by experiments using defect platforms coupling dangling bonds on a hydrogen-terminated Si(100)¹¹ (Fig. 2c), and coupling Cl vacancies in Cl/Cu(100) (Fig. 2d).¹⁴ In these systems the hopping

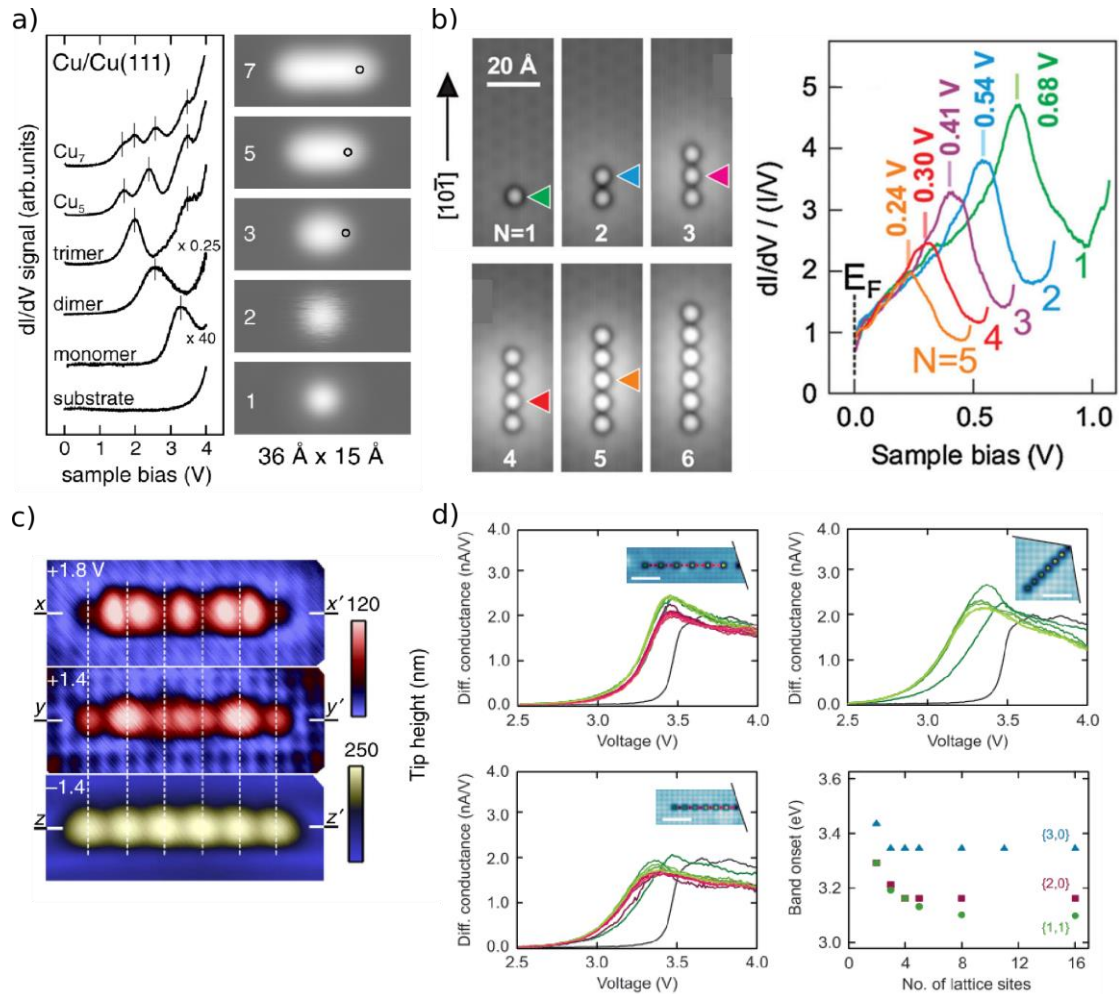


Fig. 2. Formation of quantum well states from nearest-neighbor interactions of adatoms and vacancies.

(a) Left: differential conductance spectra of chains of Cu atoms on Cu(111) (number of atoms in the chain indicated). Peaks marked by vertical bars indicate the formation of quantized states in the pseudogap of the projected Cu bulk band structure. Right: topographic images of the corresponding adatom chains. Open circles indicate the positions where the dI/dV spectra were acquired. Image taken from ref. ². (b) STM images showing the successive assembly of a In_6 chain on InAs. The coloured arrows indicate the positions where the differential conductance spectra shown in the right panel were acquired. Image adapted from ref. ⁷. (c) STM constant-current images of a chain of five closely spaced dangling bonds on the Si(100):H surface taken at the indicated voltages. Image taken from ¹¹. The changes in the pattern with energy reflect the different wave functions of the chain. (d) dI/dV spectra taken on vacancy sites and/or chlorine interstices on lattices with 16 vacancy sites for spacing configuration $\{3,0\}$ (top left), $\{2,0\}$ (bottom left) and $\{1,1\}$ (top right). $\{x,y\}$ indicates the vacancy spacing in x , and y directions, respectively. Locations where spectra were taken are indicated by coloured dots in the insets (blue: Cl atoms, black: vacancies). The bottom right panel shows how the onset of the peak depends on chain length for different configurations. Image taken from ref. ¹⁴.

parameter is controlled by the spacing of the defects. As expected from basic tight-binding considerations, a shorter lattice spacing results in a stronger hopping parameter and broader bands. The finite 1D chain features standing Bloch waves, indicative of quasiparticle bands. In case of the Cl vacancies on Cl/Cu(100), 2D lattices with different structures were studied as well and it was found that the effective electron mass strongly depends on the lattice geometry.

A breakthrough going beyond creating QWS was the realization of artificial or so-called molecular graphene, from a larger ensemble of molecules that can be arranged into 2D lattices to realize more exotic quantum states of matter.³ The conceptual idea, similar to the quantum corral, is to utilize adsorbates as scattering centres and create a periodic scattering potential pattern. The artificial graphene is the first clear example in which STM manipulation was used to create designer quantum matter (Fig. 3). For the molecular graphene, the 2DEG of the Cu(111) surface state was patterned by arranging CO molecules in a hexagonal lattice on the surface. The formation of the triangular anti-lattice creates the necessary honeycomb geometry in the 2DEG (Fig. 3a, left panel).^{3,101,102} The manifestation of molecular graphene is the appearance of a Dirac-like V-shaped LDOS (Fig. 3a, right panel). DFT calculations show that the band structure of the artificial graphene indeed features Dirac dispersion, but they are located at the Γ -point (instead of at the K-point for freestanding graphene).¹⁰² Since the electron density of the surface state is not strongly affected by the presence of adsorbates, the effective number of electrons per lattice site increases when making the unit cell larger. This allows shifting the Fermi energy relative to the Dirac point, i.e., to effectively control the level of doping in the system. Utilizing this, atomically sharp *p-n-p* junctions were created by connecting adjacent molecular graphene lattices with differing lattice constants (Fig. 3b). In addition, it becomes possible to study how strain affects the electronic structure. For graphene, strain that breaks the sublattice symmetry introduces a Gauge field, or so-called pseudo magnetic field, which modifies the electronic structure in the same way as an actual magnetic field, although pseudo magnetic fields can be realized that far exceed the highest possible real fields¹⁰³. In STM-assembled lattices of CO on Cu(111), the effect of triaxial strain on the electronic structure of artificial graphene was studied by simply modifying the arrangement of CO molecules, providing a method to experimentally study the electronic structure of graphene in pseudo magnetic fields up to $B = 60 \text{ T}$ ³.

Utilizing the aforementioned approach, it is also possible to create designer quantum materials which had not been realized previously. The most prominent example has been the realization of the Lieb

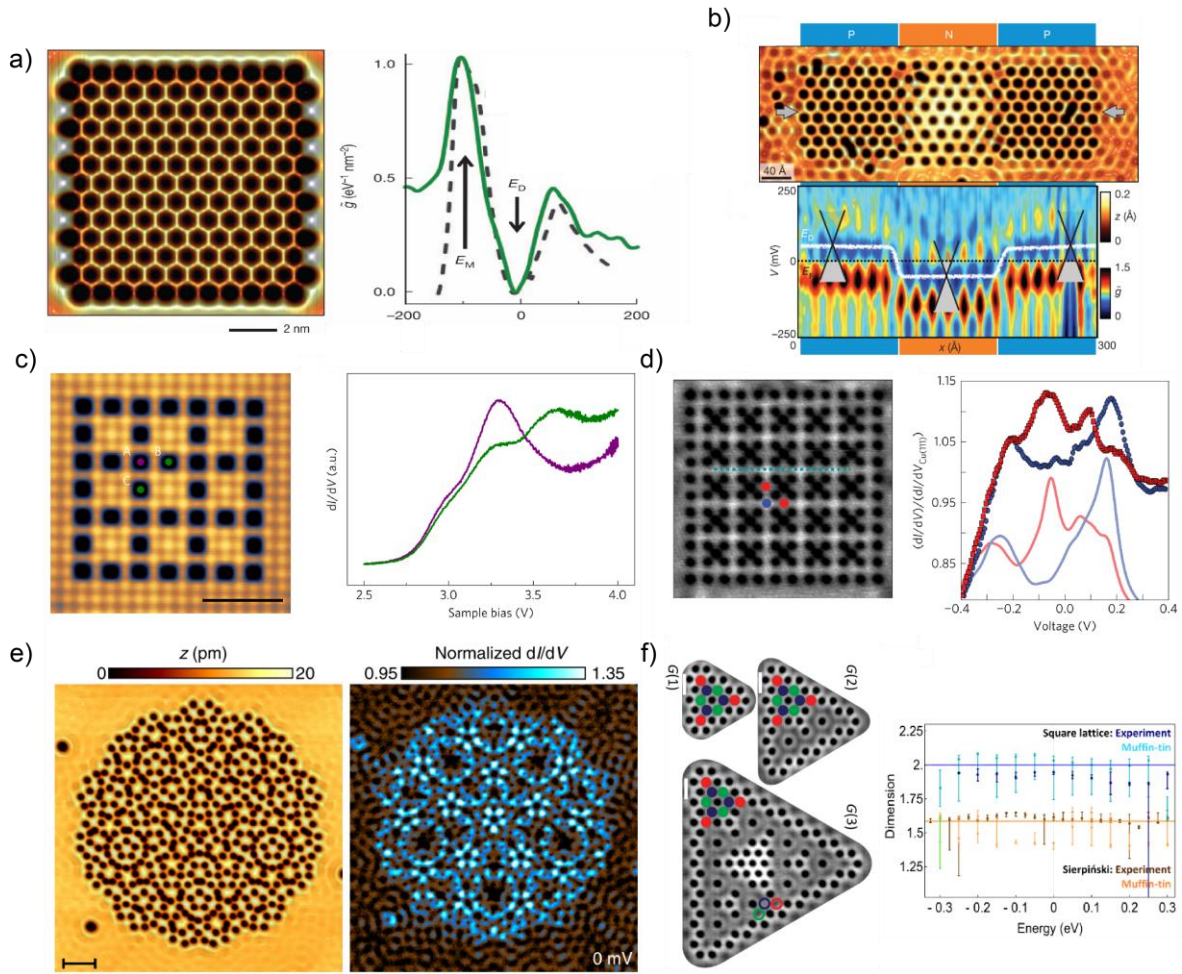


Fig. 3. Creating complex lattice structures. (a) Left: A hexagonal lattice of CO molecules (black) confines the surface state 2DEG of Cu(111) into its anti-lattice: a honeycomb geometry. Right: dI/dV spectrum (green) of the honeycomb lattice reveals a Dirac-like LDOS. Position of the Dirac cone indicated by E_D . The results are corroborated by tight-binding calculations (black dashed line). (b) Top: STM constant-current image of a hexagonal array of CO molecules on Cu(111) with two different spacings between the adsorbates. Bottom: contour plot of differential conductance spectra taken along the line indicated by the grey arrows in the top panel. The position of the Fermi level is indicated by a white line. A larger (smaller) lattice spacing corresponds to the Fermi level being located at a lower (higher) position in the band structure. (c,d) Vacancy lattices (black sites in a) (c)⁴ and 2DEGs patterned with CO molecules (black) (d)⁵ have been used to create an electronic Lieb lattice. Left panels: STM constant-current images. Right panels: dI/dV spectra taken at positions indicated by the coloured circles in the left panels, (e) Left: STM image of an arrangement of CO molecules (black) that leads to a Penrose tiling for the surface state electrons. Right panel: differential conductance map showing that the local density of states indeed exhibits a Penrose geometry. Images taken from ³⁶(f) STM images of the first three generations [G(1), G(2) and G(3)] of an electronic Sierpinski fractal. Different artificial lattice sites are indicated by different colours. Right: plot of the dimension of the electronic states of a G(3) Sierpinski lattice as determined from experimental differential conductance maps (brown) and tight-binding calculations (orange). For reference, experimental and calculated data on a square lattice is shown as well (dark and light blue, respectively). Images taken from ¹⁰⁴.

lattice, which is characterized by a Dirac dispersion, combined with a flat band at the Dirac point. The Lieb lattice in 2D is a decorated square lattice with three atoms per unit cell. Lieb lattices were created by patterning the 2DEG on the surface of Cu(111) as well as by Cl vacancies in Cl/Cu(100) (Fig. 3c,d)^{4,5}. In both cases, differential conductance spectra show a peak due to the flat band. However, these peaks are rather broad, which can be understood by non-negligible next-nearest-neighbor coupling (t_{NNN}). Interestingly, for the experiments on artificial graphene a much smaller value was found, implying that the magnitude of t_{NNN} can be tuned by modifying the pattern of CO molecules.

Patterned potentials from CO molecules on Cu(111) can also be utilized to probe electronic lattices that lack periodicity: quasicrystals and fractals. Periodicity is one of the fundamental principles underlying our understanding of the electronic structure of materials. By using CO on Cu(111), electrons have been confined to a rhombic Penrose tiling (Fig. 3e)³⁶. This quasicrystalline tiling has local order but lacks long-range periodicity. It was found that the electronic wave functions (Fig. 3e, right panel) feature the same symmetries as the geometric structure (left panel): there is rotational symmetry but no translational symmetry. The energy of the states depends on the local vertex structure of the quasicrystal. Fractals are structures that, like quasicrystals, lack periodicity and in many cases also rotational symmetry. They are self-similar on different length scales, known as expanding symmetry, and have a non-integer dimension. Physical fractals are pervasive on the macroscopic scale, but no geometric quantum fractals have been identified. Consequently, very little is known about the behaviour of electrons in non-integer dimensions. The CO on Cu(111) platform was used to create three generations of an electronic Sierpinski fractal.¹⁰⁴ These are shown in the left panel of Fig. 3f. Interestingly, the wave function inherits the dimension of the geometric structure it is confined to (right panels). The self-similarity of the fractal was found in the density of states, in the wave functions, and in reciprocal space.

Artificial electron systems are an ideal platform to test theoretical predictions regarding topology as they provide control over key variables. This is illustrated by experiments on a one-dimensional configuration of Cl vacancies in a Cl monolayer on Cu(100) with alternating weak and strong interactions.⁴ Depending on the sequence of interaction strengths, such a chain should feature topologically protected states localized at the ends of the chain with energies in the band gap.¹⁰⁵ Such states were indeed observed.⁴

Artificial spin lattices

In addition to the electronic degree of freedom, it is possible to control the spin degree of freedom by utilizing atomic adsorbates which host a magnetic moment and can be manipulated. This enables complex magnetic structures to be constructed, atom-by-atom, and to be probed by spin-sensitive techniques. In this section, we will review various lattices constructed from individual magnetic transition metal atoms, both on metal and thin insulating surfaces. The complexity of these systems ranges from Heisenberg-coupled isotropic spins³⁷ to strongly anisotropic systems displaying magnetic remanence^{45,106} as well as spiralling spin states as a result of Dzyaloshinskii-Moriya interaction⁴⁴. We will also focus on spin arrays that undergo a phase transition due to application of an external magnetic field^{6,39}.

The artificial spin lattices described here were all probed by either spin-polarized STM (SP-STM)¹⁰⁷ or inelastic electron tunnelling spectroscopy (IETS)⁴⁶, or a combination of the two (Fig. 4). These techniques can be applied either in DC mode or in sequences of pulses, giving access to time-dependent phenomena up to about 1 GHz. A commonly used pulse technique is pump-probe spectroscopy¹⁰⁸. Here, a 'pump' pulse exceeding the voltage threshold for an inelastic process is followed by a 'probe' pulse below the threshold, separated by a time duration Δt . The spin-polarized contribution due to the probe pulse causes the total current to decay as a function of Δt , revealing the lifetime of the excited state. A more recent development allows electron paramagnetic resonance (EPR) at even higher frequencies to be performed at the single atom level by means of STM¹⁰⁹, providing access to spin transitions with highly improved energy resolution. In these experiments a high-frequency signal (in the range of 20-30 GHz) is sent to the tip. If the applied frequency matches the Larmor precession of the spin being probed, a Rabi flip of the spin is induced. This, in turn, influences the time-averaged spin-polarized signal, resulting in a sharp peak (or dip) in the current exactly at the resonance frequency. As the focus of this review is on the engineering of spin lattices, we discuss these techniques to the extent that is necessary for the characterization of the interactions of the spins with their environment. A more in-depth discussion of the possibilities enabled in particular by EPR-STM is beyond the scope of this review.

The use of magnetic atoms as building blocks introduces a set of new input parameters for the design of artificial lattices. The most prominent parameters are the magnetic moment, magnetic anisotropy and

exchange-type interactions between magnetic moments. As evidenced by examples listed below, each of these can by now be adjusted with varying degrees of controllability. We will focus on four substrates that are commonly used for assembling spin structures: the metal surfaces Pt(111) and Cu(111), and the ultrathin insulators Cu₂N on Cu(100) and MgO on Ag(100) (Fig. 4).

The magnitude of the magnetic moment is determined mainly by the choice of atomic element. As the orbital moment L of 3d transition metal atoms on surfaces is typically quenched, the atomic spin moment S predominantly determines the magnitude of the total magnetic moment found on each atomic site, which we hence refer to as 'spin'. Depending on the level of hybridisation of the moment-bearing orbitals with the substrate conduction electrons, the local spin magnitude can be close to the (half-)integer value of S^{89} as derived from Hund's rules, reduced in the case of charge transfer⁴⁹, or non-half integer in the case of strong hybridization⁴⁷. In the first case, the choice of integer vs. half-integer spin magnitude has profound influence on the expected behaviour of the spin system: due to Kramer's degeneracy, half-integer spin systems are prone to display Kondo screening¹¹⁰ whereas in integer spin systems such degeneracies are easily broken by single-ion magnetic anisotropy resulting in suppressed or even absent Kondo interactions. In addition, there is the general trend that, the larger the spin, the more profound the influence of magnetic anisotropy. Spin-1/2 systems are even completely immune to magnetic anisotropy.

Magnetic anisotropy is a particularly important design parameter, often described by a typical phenomenological spin Hamiltonian¹¹¹. In situations with low anisotropy, the energy spectrum is typically governed by the Zeeman energy, leading to a ladder-like state distribution. This is the case e.g. for Mn (having $L = 0$) on Cu₂N^{37,68}. Systems with stronger uniaxial anisotropy will exhibit a more barrier-like situation, provided that the anisotropy is of the 'easy-axis' type. This is the case for e.g. Fe (adsorbed on an fcc hollow-site) on Pt(111)⁴⁷, Fe on Cu₂N⁸⁹ and Co on MgO¹¹². Conversely, if the anisotropy is of the 'easy-plane' type, states with small magnetization along the primary anisotropy axis will be favoured, e.g. in Co on Cu₂N¹¹⁰ and Fe (adsorbed on an hcp hollow-site) on Pt(111)⁴⁷.

The third input parameter to be discussed is the magnetic coupling. Depending on the environment, several physical mechanisms may lead to coupling of neighbouring spins. On metal surfaces, the primary interaction is RKKY-like coupling. The oscillatory nature as a function of distance, which is

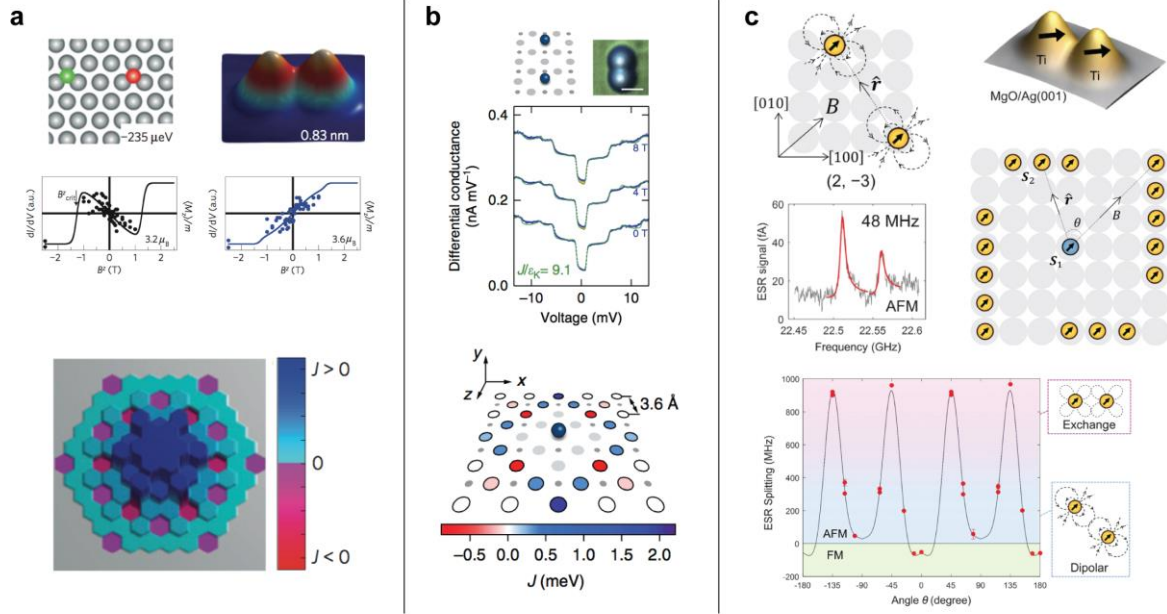


Fig. 4. Determination of spin couplings on different substrates. (a) Distance-dependent RKKY coupling of atomic Co spins on Pt(111) as measured by SP-STM¹. Top: Ball model and STM topography of an atom pair. Middle: Magnetisation curves as function of the out-of-plane applied magnetic field on the left (black) and right (blue) atom of the pair; the observed critical field is a measure for the exchange coupling J . Bottom: Calculated values of J for various atom separations. (b) Distance- and orientation-dependent superexchange coupling for two Co atoms on Cu₂N/Cu(100) acquired via spin excitation IETS⁹. Top: Ball model and STM topography of an atom pair. Middle: Differential conductance spectroscopy measurement (blue) and simulation (green) on one of the atoms in the pair. Bottom: Values of J extracted from fitting simulated spectra to measurements for various atom separations. (c) Dipole-dipole coupling of atomic Ti spins on MgO/Ag(001) determined by EPR-STM¹². Top: Ball model and STM topography of an atom pair. Middle: EPR-STM measurement taken on one atom in the pair (left); the observed splitting of the peak is a measure for J . Overview of various separations investigated, defining the coupling angle θ (right). Bottom: Observed values of J as a function of θ .

characteristic for RKKY interaction, was measured through magnetisation curves on atoms both on Cu(111)⁶ and Pt(111)¹ (Fig. 4a). On Cu₂N, RKKY coupling plays a role too, but in this case there is a competing effect of superexchange coupling through the covalent nitride network making it difficult to disentangle the two effects. Detailed analysis by means of IETS of magnetic dimers built in various orientations revealed that equal separation between the atoms can lead to completely different interaction strengths and even to sign inversion (i.e. antiferromagnetic to ferromagnetic coupling) depending on the crystallographic direction along which the atoms are positioned^{9,113} (Fig. 4b). Lastly, on MgO, spin interactions among Fe and Co atoms separated over larger distances (up to several nm)

were identified to be of dipolar nature^{92,114} (Fig. 4c). The minute μeV -scale shifts in excitation energy due to these interactions were measured via changes in the resonance frequency during an ESR measurement on one of the atoms in the pair.

By making use of the design parameters described above and by tuning their relative strengths, it becomes possible to engineer a wide scope of spin lattices that cover different coupling regimes. If for example the spin-spin coupling is chosen to be weak compared to both anisotropy and the external magnetic field, one can realize a situation where neighbouring spins only mildly perturb the local spin of an atom from their isolated state^{12,90,92}. When combined with easy-plane anisotropy, which favours states with low magnetization quantum number m_z , lattices can be created whose combined low-energy states will be made up exclusively of the low-spin subspace of each of the individual atoms. This technique was used to create an effective spin-1/2 chain from actual spin-3/2 Co atoms on Cu_2N ³⁹. If, on the other hand, this approach is employed in conjunction with easy-axis anisotropy, only the large m_z states enter the low-energy spectrum of the lattice. In such cases, the transverse components of the Heisenberg coupling $J(S_x S_x + S_y S_y) = J/2(S_+ S_- + S_- S_+)$ do not to first order couple the states, resulting in a situation that can be effectively described as Ising coupling $J S_z S_z$. Such systems are ideal for probing by means of spin-polarized STM, as the favoured states all have maximum magnetization parallel or anti-parallel to the tip polarization. This technique was used successfully to visualize the transition between various magnetization states in antiferromagnetic and frustrated spin structures which were driven through a phase transition by an external magnetic field⁶ (Fig. 5a). This regime was also employed for realizing a logic gate based on antiferromagnetic leads, where the magnetization states of the leads were fixed by large Co islands that served as input gates³⁸.

When the spin-spin coupling and magnetic anisotropy are chosen to be of comparable strength, a situation arises where the anisotropies of neighbouring atoms reinforce each other. Provided that the anisotropy is easy-axis, this will result in a pair of bistable states that are separated by an energy barrier. The height of this barrier, which determines the switching rate between the two states, depends on the number of spins, their spin magnitudes, their anisotropies and their couplings. Switching rates of 1 Hz and lower were observed for both ferromagnetic¹¹⁵ and antiferromagnetic⁴⁵ Fe chains in Cu_2N (Fig. 5b), and for ferromagnetic arrays on $\text{Cu}(111)$ ¹⁰⁶ and $\text{Pt}(111)$ ¹¹⁶.

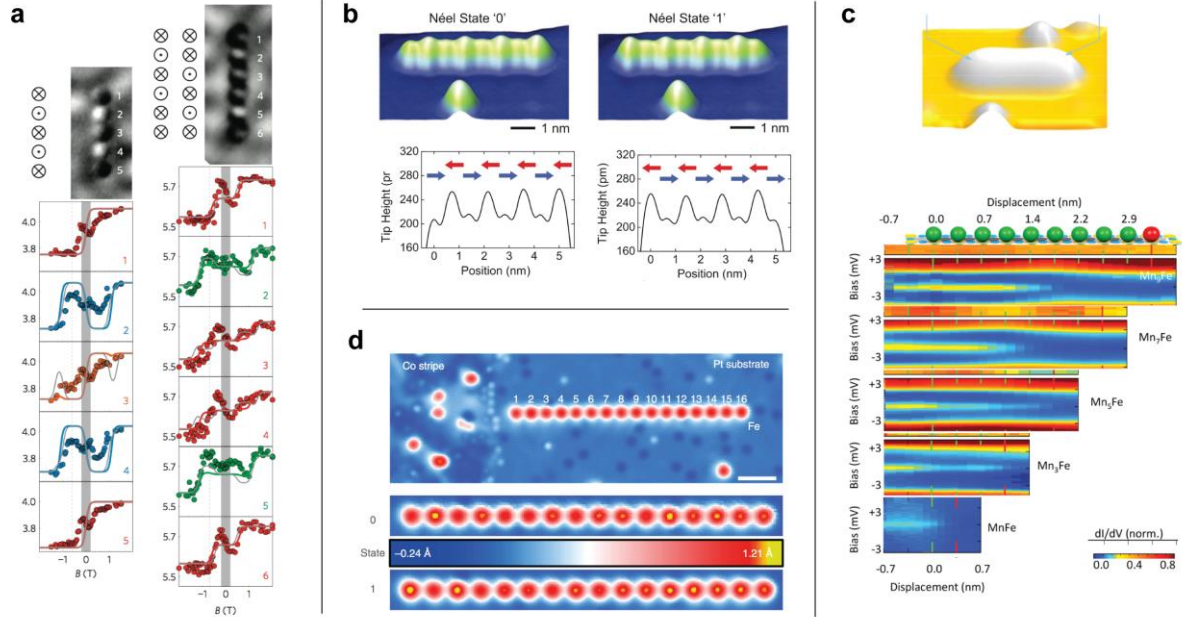


Fig. 5. Spin chains built in three different coupling regimes. (a) SP-STM images (top) and corresponding single-atom magnetization curves (bottom) of a 5- and a 6-atom Fe chain on Cu(111)⁶. Colours and arrow diagrams show interpretation of the local magnetisation from the SP-STM contrast. (b) SP-STM images (top) and cross-sections (bottom) of an 8-atom Fe chain on Cu₂N/Cu(100) which can be switched between two stable Néel states⁴⁵. Arrows show interpretation of the local magnetisation from the SP-STM contrast. (c) STM constant-current image (top), ball model (middle) and spectroscopic maps (bottom) of a Mn_xFe entangled spin chains on Cu₂N/Cu(100) showing the spatial evolution of Kondo screening¹¹⁷. (d) STM (top) and SP-STM (bottom) images of a 16-atom Fe chain coupled to a Co stripe on Pt(111), showing non-collinear spin states⁴⁴.

The final coupling regime we will discuss is the case where the spin-spin coupling is much stronger than the magnetic anisotropy energy. Spin chains in this regime are often well-described by the giant spin approximation. Spectroscopy in this case typically does not vary from atom to atom but rather describes the excitations of the chain as a whole³⁷. Spin chains in this coupling regime were demonstrated to provide a testbed for studying the two-site Kondo effect as a function of separation distance¹¹⁸. More recently, spin chains in this coupling regime were locally doped with a single spin of a different magnitude, providing an opportunity for measuring long-range spin correlation and delocalization effects in extended spin states¹¹⁷ (Fig. 5c).

The coupling mechanisms discussed so far, be it RKKY, superexchange or dipolar interaction, are all collinear couplings and can be expressed in the form of Heisenberg exchange. An additional, non-collinear interaction was found between Fe atoms on Pt(111) (Fig. 5d). This Dzyaloshinskii-Moriya (DM)

interaction results from strong spin-orbit coupling with the heavy substrate atoms combined with broken inversion symmetry at the surface. Recently it was shown that the DM interaction can be utilized to engineer spin spirals in sufficiently long chains of spins⁴⁴, and provides an interesting additional degree of freedom to create 2D topological magnets, bottom-up, as well as non-collinear magnets on superconductors¹¹⁹.

Conclusion and Outlook

In conclusion, STM can serve as a complete nanoscale lab in which both electronic and magnetic structures can be tailored, atom-by-atom, and subsequently characterized with unprecedented resolution. This enables the construction of novel states of matter, such as Dirac and topologically non-trivial materials which are difficult to engineer³⁻⁵, as well as quasicrystals³⁶ and electronic fractals¹⁰⁴. Moreover, complex magnetic order can be tailored bottom-up^{6,39,44}, and their static and dynamic properties probed with single atom resolution. One important aspect to mention, is the effect of finite size. This was studied systematically for 1D and 2D Cl vacancy lattices, as well as for CO on Cu(111)^{5,14}. Surprisingly, finite-size effects are no longer significant for band onsets in Cl-vacancy lattices as small as 8x8 as well as for resonance energies in CO on Cu(111) 5x5 unit cells. Furthermore, similar effects are an important consideration for the development of magnetic order in artificial spin systems, and have been studied in detail in spin chain systems^{6,39}.

Artificial lattices are promising for studying a variety of complex phenomena, where atomic-scale control of interactions is highly desired toward new theoretical understandings. New potential systems are also emerging, which may serve as new platforms for artificial lattices^{92,120}. A natural extension of studying artificial electronic lattices is to look at higher orbital band engineering¹²¹. This is especially intriguing when spin-orbit coupling is introduced in artificial lattices¹²². Another natural avenue for future exploration is studying topology. Topologically non-trivial states are protected by symmetries of the system. Artificial lattice systems allow for sequentially and selectively breaking all symmetries of the lattice. This platform is therefore ideally suited to experimentally test the protection mechanisms and robustness of topological states. As discussed above, the 1D Su-Schrieffer-Heeger (SSH) model has already been realized by coupling Cl vacancy states^{4,123}. For the CO/Cu(111) platform, the interaction strength (hopping parameter) between artificial lattice sites can be tuned by controlling the

number and arrangement of the CO molecules that define the boundary between the sites. This approach was used to create a higher order crystalline topological insulator based on the Kagomé lattice¹²⁴. In this lattice, the non-trivial states were found to be localized at the corners of the 2D lattice.

In a similar manner, manipulated spin structures on superconductors is a preferred route toward understanding Majorana zero modes created from engineered magnetic structures on BCS superconductors¹²⁵, and a route toward tailoring topological superconductivity¹¹⁹. While 1D bottom-up magnetic chains on superconductors are being explored, 2D artificial lattices could also potentially be created¹²⁶. In a similar manner, 2D chiral magnets could be potentially engineered bottom-up⁴⁴, to realize isolated topological magnets. For example, it may be conceivable to construct isolated skyrmions with tailored order¹²⁷. Very recent work suggests that it is possible to study heavy-fermion physics by coupling Kondo droplets created by positioning Co atoms on Cu(111)¹²⁸.

Moreover, all electronic lattice studies based on STM, to date, are well described within single-particle pictures, and based on tight-binding or muffin-tin approaches^{5,101,104,121}. Several other approaches which employ a bottom-up philosophy, such as magic-angle moiré engineering^{18,19}, cold atoms⁸, optical lattices^{16,17}, and engineered quantum dots¹⁵ have studied many-body ground states driven by electron-electron interactions. Being able to tailor correlated electron effects in artificial lattice systems, atom-by-atom, would be an extremely promising platform for studying emergent ground states, and an essential approach to develop in order to push the artificial lattice platform based on STM methods to compete with other established methods.

Finally, with the development of high temporal resolution techniques^{108,109}, it will be interesting to study spin and charge dynamics in coupled lattice systems in which hopping can be tailored, as well as magnetic interactions. For example, many-body quantum spin states could potentially be manipulated with microwave or optical methods, by spin resonance¹⁰⁹ or pump-probe methods^{108,129}, as an outlet for quantum computing. Similarly, the formation of spin frustration as well as glass-like behaviour would be an ideal platform to study the static and dynamic behaviour of spin glasses¹³⁰ as well as new directions in stochastic and brain-inspired computing¹³¹.

Acknowledgements

AAK would like to acknowledge NWO-VIDI project: “Manipulating the interplay between superconductivity and chiral magnetism at the single-atom level” with project number 680-47-534, and

funding from the European Research Council (ERC) under the European Union's Horizon 2020 research and innovation programme (grant agreement No. 818399 'SPINAPSE'). AFO acknowledges support from the European Research Council (ERC Starting Grant 676895 'SPINCAD'). IS acknowledges funding from NWO (grant number 16PR3245-1).

References

- 1 Zhou, L. *et al.* Strength and directionality of surface Ruderman–Kittel–Kasuya–Yosida interaction mapped on the atomic scale. *Nature Physics* **6**, 187 (2010).
- 2 Fölsch, S., Hyldgaard, P., Koch, R. & Ploog, K. H. Quantum Confinement in Monatomic Cu Chains on Cu(111). *Physical Review Letters* **92**, 056803 (2004).
- 3 Gomes, K. K., Mar, W., Ko, W., Guinea, F. & Manoharan, H. C. Designer Dirac fermions and topological phases in molecular graphene. *Nature* **483**, 306 (2012).
- 4 Drost, R., Ojanen, T., Harju, A. & Liljeroth, P. Topological states in engineered atomic lattices. *Nature Physics* **13**, 668 (2017).
- 5 Slot, M. R. *et al.* Experimental realization and characterization of an electronic Lieb lattice. *Nature Physics* **13**, 672 (2017).
- 6 Khajetoorians, A. A. *et al.* Atom-by-atom engineering and magnetometry of tailored nanomagnets. *Nature Physics* **8**, 497-503 (2012).
- 7 Fölsch, S., Yang, J., Nacci, C. & Kanisawa, K. Atom-By-Atom Quantum State Control in Adatom Chains on a Semiconductor. *Physical Review Letters* **103**, 096104 (2009).
- 8 Bloch, I., Dalibard, J. & Nascimbène, S. Quantum simulations with ultracold quantum gases. *Nature Physics* **8**, 267 (2012).
- 9 Spinelli, A. *et al.* Exploring the phase diagram of the two-impurity Kondo problem. *Nature Communications* **6** (2015).
- 10 Blatt, R. & Roos, C. F. Quantum simulations with trapped ions. *Nature Physics* **8**, 277 (2012).
- 11 Schofield, S. R. *et al.* Quantum engineering at the silicon surface using dangling bonds. *Nature Communications* **4**, 1649 (2013).
- 12 Yang, K. *et al.* Engineering the Eigenstates of Coupled Spin- $1/2$ Atoms on a Surface. *Physical Review Letters* **119**, 227206 (2017).
- 13 Houck, A. A., Türeci, H. E. & Koch, J. On-chip quantum simulation with superconducting circuits. *Nature Physics* **8**, 292 (2012).
- 14 Girovsky, J. *et al.* Emergence of quasiparticle Bloch states in artificial crystals crafted atom-by-atom. *SciPost Physics* **2**, 020 (2017).
- 15 Singha, A. *et al.* Two-Dimensional Mott-Hubbard Electrons in an Artificial Honeycomb Lattice. *Science* **332**, 1176 (2011).
- 16 Bloch, I. Ultracold quantum gases in optical lattices. *Nature Physics* **1**, 23 (2005).
- 17 Gross, C. & Bloch, I. Quantum simulations with ultracold atoms in optical lattices. *Science* **357**, 995 (2017).
- 18 Cao, Y. *et al.* Correlated insulator behaviour at half-filling in magic-angle graphene superlattices. *Nature* **556**, 80 (2018).
- 19 Cao, Y. *et al.* Unconventional superconductivity in magic-angle graphene superlattices. *Nature* **556**, 43 (2018).
- 20 Barth, J. V. Molecular architectonic on metal surfaces. *Annu Rev Phys Chem* **58**, 375-407 (2007).
- 21 Elemans, J. A. A. W., Lei, S. B. & De Feyter, S. Molecular and Supramolecular Networks on Surfaces: From Two-Dimensional Crystal Engineering to Reactivity. *Angew Chem Int Edit* **48**, 7298-7332 (2009).
- 22 Lackinger, M. On-surface polymerization - a versatile synthetic route to two-dimensional polymers. *Polym Int* **64**, 1073-1078 (2015).
- 23 Dong, L., Gao, Z. A. & Lin, N. Self-assembly of metal-organic coordination structures on surfaces. *Progress in Surface Science* **91**, 101-135 (2016).
- 24 Klappenberger, F. *et al.* Dichotomous Array of Chiral Quantum Corrals by a Self-Assembled Nanoporous Kagome Network. *Nano Letters* **9**, 3509-3514 (2009).

- 25 Lobo-Checa, J. *et al.* Band Formation from Coupled Quantum Dots Formed by a Nanoporous
Network on a Copper Surface. *Science* **325**, 300-303 (2009).
- 26 Shang, J. *et al.* Assembling molecular Sierpinski triangle fractals. *Nat Chem* **7**, 389-393
(2015).
- 27 Piquero-Zulaica, I. *et al.* Precise engineering of quantum dot array coupling through their
barrier widths. *Nature Communications* **8** (2017).
- 28 Cheng, F. *et al.* Two-dimensional tessellation by molecular tiles constructed from halogen-
halogen and halogen-metal networks. *Nature Communications* **9** (2018).
- 29 Stepanow, S. *et al.* Steering molecular organization and host-guest interactions using two-
dimensional nanoporous coordination systems. *Nature Materials* **3**, 229-233 (2004).
- 30 Schlickum, U. *et al.* Metal-organic honeycomb nanomeshes with tunable cavity size. *Nano
Letters* **7**, 3813-3817 (2007).
- 31 Li, C. *et al.* Construction of Sierpinski Triangles up to the Fifth Order. *Journal of the American
Chemical Society* **139**, 13749-13753 (2017).
- 32 Grill, L. *et al.* Nano-architectures by covalent assembly of molecular building blocks. *Nature
Nanotechnology* **2**, 687-691 (2007).
- 33 Eichhorn, J. *et al.* On-Surface Ullmann Coupling: The Influence of Kinetic Reaction
Parameters on the Morphology and Quality of Covalent Networks. *Acs Nano* **8**, 7880-7889
(2014).
- 34 Rizzo, D. J. *et al.* Topological band engineering of graphene nanoribbons. *Nature* **560**, 204-
208 (2018).
- 35 Gröning, O. *et al.* Engineering of robust topological quantum phases in graphene nanoribbons.
Nature **560**, 209-213 (2018).
- 36 Collins, L. C., Witte, T. G., Silverman, R., Green, D. B. & Gomes, K. K. Imaging quasiperiodic
electronic states in a synthetic Penrose tiling. *Nature Communications* **8**, 15961 (2017).
- 37 Hirjibehedin, C. F., Lutz, C. P. & Heinrich, A. J. Spin coupling in engineered atomic structures.
Science **312**, 1021-1024 (2006).
- 38 Khajetoorians, A. A., Wiebe, J., Chilian, B. & Wiesendanger, R. Realizing All-Spin-Based
Logic Operations Atom by Atom. *Science* **332**, 1062-1064 (2011).
- 39 Toskovic, R. *et al.* Atomic spin-chain realization of a model for quantum criticality. *Nature
Physics* **12**, 656 (2016).
- 40 Serrate, D. *et al.* Imaging and manipulating the spin direction of individual atoms. *Nature
Nanotechnology* **5**, 350 (2010).
- 41 Song, Y. J. *et al.* High-resolution tunnelling spectroscopy of a graphene quartet. *Nature* **467**,
185 (2010).
- 42 Kalff, F. E. *et al.* A kilobyte rewritable atomic memory. *Nature Nanotechnology* **11**, 926 (2016).
- 43 Crommie, M. F., Lutz, C. P. & Eigler, D. M. Confinement of Electrons to Quantum Corrals on a
Metal-Surface. *Science* **262**, 218-220 (1993).
- 44 Steinbrecher, M. *et al.* Non-collinear spin states in bottom-up fabricated atomic chains. *Nature
Communications* **9**, 2853 (2018).
- 45 Loth, S., Baumann, S., Lutz, C. P., Eigler, D. M. & Heinrich, A. J. Bistability in Atomic-Scale
Antiferromagnets. *Science* **335**, 196-199 (2012).
- 46 Heinrich, A. J., Gupta, J. A., Lutz, C. P. & Eigler, D. M. Single-atom spin-flip spectroscopy.
Science **306**, 466-469 (2004).
- 47 Khajetoorians, A. A. *et al.* Spin Excitations of Individual Fe Atoms on Pt(111): Impact of the
Site-Dependent Giant Substrate Polarization. *Physical Review Letters* **111**, 157204 (2013).
- 48 Khajetoorians, A. A. *et al.* Itinerant nature of atom-magnetization excitation by tunneling
electrons. *Physical Review Letters* **106**, 037205 (2011).
- 49 Khajetoorians, A. A. *et al.* Detecting excitation and magnetization of individual dopants in a
semiconductor. *Nature* **467**, 1084-1087 (2010).
- 50 Celotta, R. J. *et al.* Invited Article: Autonomous assembly of atomically perfect nanostructures
using a scanning tunneling microscope. *Review of Scientific Instruments* **85**, 121301-121301
(2014).
- 51 Eigler, D. M. & Schweizer, E. K. Positioning single atoms with a scanning tunneling
microscope. *Nature* **344**, 524-526 (1990).
- 52 Chen, C. J. *Introduction to Scanning Tunneling Microscopy*. second edition edn, (Oxford
University Press, 2015).
- 53 Voigtländer, B. *Scanning Probe Microscopy*. (Springer, 2015).
- 54 Song, Y. J. *et al.* Invited Review Article: A 10 mK scanning probe microscopy facility. *Review
of Scientific Instruments* **81**, 121101 (2010).

- 55 Assig, M. *et al.* A 10 mK scanning tunneling microscope operating in ultra high vacuum and
high magnetic fields. *Review of Scientific Instruments* **84**, 033903 (2013).
- 56 Misra, S. *et al.* Design and performance of an ultra-high vacuum scanning tunneling
microscope operating at dilution refrigerator temperatures and high magnetic fields. *Review of
Scientific Instruments* **84**, 103903 (2013).
- 57 von Allwörden, H. *et al.* Design and performance of an ultra-high vacuum scanning tunneling
microscope operating at 30 mK and in a vector magnetic field. *Review of Scientific
Instruments* **89**, 033902 (2018).
- 58 Roychowdhury, A. *et al.* A 30 mK, 13.5 T scanning tunneling microscope with two independent
tips. *Review of Scientific Instruments* **85**, 043706 (2014).
- 59 Machida, T., Kohsaka, Y. & Hanaguri, T. A scanning tunneling microscope for spectroscopic
imaging below 90 mK in magnetic fields up to 17.5 T. *Review of Scientific Instruments* **89**,
093707 (2018).
- 60 Balashov, T., Meyer, M. & Wulfhekel, W. A compact ultrahigh vacuum scanning tunneling
microscope with dilution refrigeration. *Review of Scientific Instruments* **89**, 113707 (2018).
- 61 Lorente, N. & Persson, M. Theory of single molecule vibrational spectroscopy and microscopy.
Physical Review Letters **85**, 2997-3000 (2000).
- 62 Lorente, N., Persson, M., Lauhon, L. J. & Ho, W. Symmetry selection rules for vibrationally
inelastic tunneling. *Physical Review Letters* **86**, 2593-2596 (2001).
- 63 Ternes, M. Probing magnetic excitations and correlations in single and coupled spin systems
with scanning tunneling spectroscopy. *Progress in Surface Science* **92**, 83-115 (2017).
- 64 Stipe, B. C., Rezaei, M. A. & Ho, W. Single-molecule vibrational spectroscopy and
microscopy. *Science* **280**, 1732-1735 (1998).
- 65 Vitali, L., Schneider, M. A., Kern, K., Wirtz, L. & Rubio, A. Phonon and plasmon excitation in
inelastic electron tunneling spectroscopy of graphite. *Physical Review B* **69**, 121414 (2004).
- 66 Gawronski, H., Mehlhorn, M. & Morgenstern, K. Imaging Phonon Excitation with Atomic
Resolution. *Science* **319**, 930 (2008).
- 67 Gao, C. L. *et al.* Spin Wave Dispersion on the Nanometer Scale. *Physical Review Letters* **101**,
167201 (2008).
- 68 Loth, S. *et al.* Controlling the state of quantum spins with electric currents. *Nature Physics* **6**,
340 (2010).
- 69 Wiesendanger, R. Spin mapping at the nanoscale and atomic scale. *Reviews of Modern
Physics* **81**, 1495-1495 (2009).
- 70 Bode, M. Spin-polarized scanning tunnelling microscopy. *Reports on Progress in Physics* **66**,
523 (2003).
- 71 Bartels, L., Meyer, G. & Rieder, K. H. Basic Steps of Lateral Manipulation of Single Atoms and
Diatomic Clusters with a Scanning Tunneling Microscope Tip. *Physical Review Letters* **79**,
697-697 (1997).
- 72 Ternes, M., Lutz, C. P., Hirjibehedin, C. F., Giessibl, F. J. & Heinrich, A. J. The force needed
to move an atom on a surface. *Science* **319**, 1066-1069 (2008).
- 73 Hla, S. W. Atom-by-atom assembly. *Reports on Progress in Physics* **77** (2014).
- 74 Crommie, M. F., Lutz, C. P. & Eigler, D. M. Confinement of Electrons to Quantum Corrals on a
Metal Surface. *Science* **262**, 218 (1993).
- 75 Eigler, D. M., Lutz, C. P. & Rudge, W. E. An atomic switch realized with the scanning
tunneling microscope. *Nature* **352**, 600-603 (1991).
- 76 Bartels, L., Meyer, G. & Rieder, K. H. Controlled vertical manipulation of single CO molecules
with the scanning tunneling microscope: A route to chemical contrast. *Applied Physics Letters*
71, 213-215 (1997).
- 77 Swart, I., Sonleitner, T., Niedenführ, J. & Repp, J. Controlled Lateral Manipulation of
Molecules on Insulating Films by STM. *Nano Letters* **12**, 1070-1074 (2012).
- 78 Shen, T. C. *et al.* Atomic-Scale Desorption through Electronic and Vibrational-Excitation
Mechanisms. *Science* **268**, 1590-1592 (1995).
- 79 Albrecht, F., Neu, M., Quest, C., Swart, I. & Repp, J. Formation and characterization of a
molecule-metal-molecule bridge in real space. *Journal of the American Chemical Society* **135**,
9200-9203 (2013).
- 80 Custance, O., Perez, R. & Morita, S. Atomic force microscopy as a tool for atom manipulation.
Nature Nanotechnology **4**, 803-810 (2009).
- 81 Dujardin, G. & Mayne, A. J. in *Frontiers in Nanoscience* 190 (Elsevier, Amsterdam, 2011).
- 82 Tseng, A. A. & Li, Z. Manipulations of atoms and molecules by scanning probe microscopy. *J
Nanosci Nanotechno* **7**, 2582-2595 (2007).

- 83 Hla, S. W. Scanning tunneling microscopy single atom/molecule manipulation and its
application to nanoscience and technology. *J Vac Sci Technol B* **23**, 1351-1360 (2005).
- 84 Schuler, B. *et al.* Effect of electron-phonon interaction on the formation of one-dimensional
electronic states in coupled Cl vacancies. *Physical Review B* **91** (2015).
- 85 Crommie, M. F., Lutz, C. P. & Eigler, D. M. Imaging Standing Waves in a 2-Dimensional
Electron-Gas. *Nature* **363**, 524-527 (1993).
- 86 Hasegawa, Y. & Avouris, P. Direct observation of standing wave formation at surface steps
using scanning tunneling spectroscopy. *Physical Review Letters* **71**, 1071-1074 (1993).
- 87 Heller, E. J., Crommie, M. F., Lutz, C. P. & Eigler, D. M. Scattering and absorption of surface
electron waves in quantum corrals. *Nature* **369**, 464 (1994).
- 88 Hermenau, J. *et al.* A gateway towards non-collinear spin processing using three-atom
magnets with strong substrate coupling. *Nature Communications* **8**, 642 (2017).
- 89 Hirjibehedin, C. F. *et al.* Large magnetic anisotropy of a single atomic spin embedded in a
surface molecular network. *Science* **317**, 1199-1203 (2007).
- 90 Otte, A. F. *et al.* Spin Excitations of a Kondo-Screened Atom Coupled to a Second Magnetic
Atom. *Physical Review Letters* **103**, 107203 (2009).
- 91 Meier, F., Zhou, L., Wiebe, J. & Wiesendanger, R. Revealing magnetic interactions from
single-atom magnetization curves. *Science* **320**, 82-86 (2008).
- 92 Choi, T. *et al.* Atomic-scale sensing of the magnetic dipolar field from single atoms. *Nature
Nanotechnology* **12**, 420 (2017).
- 93 Manoharan, H. C., Lutz, C. P. & Eigler, D. M. Quantum mirages formed by coherent projection
of electronic structure. *Nature* **403**, 512 (2000).
- 94 Nilius, N., Wallis, T. M. & Ho, W. Development of One-Dimensional Band Structure in Artificial
Gold Chains. *Science* **297**, 1853 (2002).
- 95 Nilius, N., Wallis, T. M. & Ho, W. Tailoring electronic properties of atomic chains assembled by
STM. *Applied Physics A* **80**, 951-956 (2005).
- 96 Nilius, N., Wallis, T. M. & Ho, W. Building Alloys from Single Atoms: Au-Pd Chains on
NiAl(110). *The Journal of Physical Chemistry B* **108**, 14616-14619 (2004).
- 97 Nilius, N., Wallis, T. M., Persson, M. & Ho, W. Interplay between Electronic Properties and
Interatomic Spacing in Artificial Gold Chains on NiAl(110). *The Journal of Physical Chemistry
C* **118**, 29001-29006 (2014).
- 98 Matsui, T., Meyer, C., Sacharow, L., Wiebe, J. & Wiesendanger, R. Electronic states of Fe
atoms and chains on InAs(110) from scanning tunneling spectroscopy. *Physical Review B* **75**,
165405 (2007).
- 99 Sperl, A. *et al.* Unoccupied states of individual silver clusters and chains on Ag(111). *Physical
Review B* **77**, 085422 (2008).
- 100 Crain, J. N. & Pierce, D. T. End States in One-Dimensional Atom Chains. *Science* **307**, 703
(2005).
- 101 Park, C.-H. & Louie, S. G. Making Massless Dirac Fermions from a Patterned Two-
Dimensional Electron Gas. *Nano Letters* **9**, 1793-1797 (2009).
- 102 Paavilainen, S., Ropo, M., Nieminen, J., Akola, J. & Räsänen, E. Coexisting Honeycomb and
Kagome Characteristics in the Electronic Band Structure of Molecular Graphene. *Nano Letters*
16, 3519-3523 (2016).
- 103 Castro Neto, A. H., Guinea, F., Peres, N. M. R., Novoselov, K. S. & Geim, A. K. Electronic
Properties of Graphene. *Reviews of Modern Physics* **81**, 109-162 (2009).
- 104 Kempkes, S. N. *et al.* Design and characterization of electrons in a fractal geometry. *Nature
Physics* (2018).
- 105 Heeger, A. J., Kivelson, S., Schrieffer, J. R. & Su, W. P. Solitons in conducting polymers.
Reviews of Modern Physics **60**, 781-850 (1988).
- 106 Khajetoorians, A. A. *et al.* Current-driven spin dynamics of artificially constructed quantum
magnets. *Science* **339**, 55-59 (2013).
- 107 Kubetzka, A., Bode, M., Pietzsch, O. & Wiesendanger, R. Spin-polarized scanning tunneling
microscopy with antiferromagnetic probe tips. *Physical Review Letters* **88** (2002).
- 108 Loth, S., Etzkorn, M., Lutz, C. P., Eigler, D. M. & Heinrich, A. J. Measurement of Fast Electron
Spin Relaxation Times with Atomic Resolution. *Science* **329**, 1628-1630 (2010).
- 109 Baumann, S. *et al.* Electron paramagnetic resonance of individual atoms on a surface.
Science **350**, 417-420 (2015).
- 110 Otte, A. F. *et al.* The role of magnetic anisotropy in the Kondo effect. *Nature Physics* **4**, 847-
850 (2008).

- 111 Fernández-Rossier, J. Theory of Single-Spin Inelastic Tunneling Spectroscopy. *Physical Review Letters* **102**, 256802 (2009).
- 112 Rau, I. G. *et al.* Reaching the magnetic anisotropy limit of a 3d metal atom. *Science* **344**, 988-992 (2014).
- 113 Bryant, B., Spinelli, A., Wagenaar, J. J. T., Gerrits, M. & Otte, A. F. Local Control of Single Atom Magnetocrystalline Anisotropy. *Physical Review Letters* **111** (2013).
- 114 Natterer, F. D. *et al.* Reading and writing single-atom magnets. *Nature* **543**, 226-228 (2017).
- 115 Spinelli, A., Bryant, B., Delgado, F., Fernández-Rossier, J. & Otte, A. F. Imaging of spin waves in atomically designed nanomagnets. *Nature Materials* **13**, 782-785 (2014).
- 116 Hermenau, J., Ternes, M., Steinbrecher, M., Wiesendanger, R. & Wiebe, J. Long Spin-Relaxation Times in a Transition-Metal Atom in Direct Contact to a Metal Substrate. *Nano Letters* **18**, 1978-1983 (2018).
- 117 Choi, D. J. *et al.* Building Complex Kondo Impurities by Manipulating Entangled Spin Chains. *Nano Letters* **17**, 6203-6209 (2017).
- 118 Neel, N. *et al.* Two-Site Kondo Effect in Atomic Chains. *Physical Review Letters* **107** (2011).
- 119 Kim, H. *et al.* Toward tailoring Majorana bound states in artificially constructed magnetic atom chains on elemental superconductors. *Science Advances* **4** (2018).
- 120 Kiraly, B. *et al.* An orbitally derived single-atom magnetic memory. *Nature Communications* **9**, 3904 (2018).
- 121 Slot, M. R. *et al.* s -Band Engineering in Artificial Electronic Lattices. *Physical Review X* **9**, 011009 (2019).
- 122 Steinbrecher, M., Harutyunyan, H., Ast, C. R. & Wegner, D. Rashba-type spin splitting from interband scattering in quasiparticle interference maps. *Physical Review B* **87** (2013).
- 123 Nurul Huda, M., Kezilebieke, S., Ojanen, T., Drost, R. & Liljeroth, P. Tuneable topological domain wall states in engineered atomic chains. *eprint arXiv:1806.08614*, arXiv:1806.08614 (2018).
- 124 Kempkes, S. N. *et al.* Robust zero-energy modes in an electronic higher-order topological insulator: the dimerized Kagome lattice. *eprint arXiv:1905.06053*, arXiv:1905.06053 (2019).
- 125 Nadj-Perge, S. *et al.* Observation of Majorana fermions in ferromagnetic atomic chains on a superconductor. *Science* **346**, 602 (2014).
- 126 Röntynen, J. & Ojanen, T. Topological Superconductivity and High Chern Numbers in 2D Ferromagnetic Shiba Lattices. *Physical Review Letters* **114**, 236803 (2015).
- 127 Romming, N. *et al.* Writing and Deleting Single Magnetic Skyrmions. *Science* **341**, 636 (2013).
- 128 Figgins, J. *et al.* Quantum Engineered Kondo Lattices. *arXiv:1902.04680* (2019).
- 129 Cocker, T. L., Peller, D., Yu, P., Repp, J. & Huber, R. Tracking the ultrafast motion of a single molecule by femtosecond orbital imaging. *Nature* **539**, 263 (2016).
- 130 Edwards, S. F. & Anderson, P. W. Theory of spin glasses. *Journal of Physics F: Metal Physics* **5**, 965 (1975).
- 131 Grollier, J., Querlioz, D. & Stiles, M. D. Spintronic Nanodevices for Bioinspired Computing. *Proceedings of the IEEE. Institute of Electrical and Electronics Engineers* **104**, 2024-2039 (2016).